Journal of Applied Polymer Science

A Physical Strategy for the Preparation of Isotactic Polypropylene Spheres with Microsphere and Bead-String Spherulite Morphologies

Jing Jin,[1] Jiang Du,[2] Hongyu Chen,[3] Gary Marchand,[4] Kim Walton,[4] Charles C. Han[5]

[1]Department of Fire Protection Engineering, Chinese People's Armed Police Forces Academy, Langfang, Hebei 065000, People's Republic of China

[2]School of Materials Science and Engineering, Tongji University, Shanghai 201804, People's Republic of China

[3]The Dow Chemical Company Limited, Shanghai 201203, People's Republic of China

[4]The Dow Chemical Company, Freeport, Texas 77541

[5]Beijing National Laboratory for Molecular Sciences, Joint Laboratory of Polymer Science and Materials, Institute of Chemistry, Chinese Academy of Sciences, Beijing 100190, People's Republic of China

Correspondence to: C. C. Han (E-mail: c.c.han@iccas.ac.cn)

ABSTRACT: This study mainly focuses on the formation of isotactic polypropylene (iPP) blend morphologies with microspheres and distinct bead–string spherulites. iPP microspheres have been prepared by a simple and convenient strategy through either an isothermal or a nonisothermal crystallization process based on the macrophase-separated structure in molten state of iPP/olefin block copolymer (OBC) blend. The dimension of the iPP spheres can be adjusted easily from about 1 μm to >10 μm by controlling the compatibility and annealing conditions. It was found that any of the following three parameters, the molecular structure of OBC (particularly the octene content), molecular weight of iPP, and annealing condition can be rescaled with others in controlling the dimension of the iPP microspheres. The mechanism of the formation of iPP microspheres was studied in detail. Surprisingly, the typical spinodal decomposition morphology with interconnected or thin sheet structure is the precursor of these microspheres. During the subsequent annealing process, it breaks up and further coarsens into spherical structure. In addition, distinct spherulites with a bead–string substructure have been obtained during the isothermal crystallization. © 2014 Wiley Periodicals, Inc. J. Appl. Polym. Sci. **2014**, *131*, 40863.

KEYWORDS: blends; crystallization; morphology; phase behavior

Received 18 December 2013; accepted 13 April 2014
DOI: 10.1002/app.40863

INTRODUCTION

Blending is indeed a convenient and efficient route for the development of new materials benefiting from a synergetic effect from the individual components.[1,2] Polyolefin blends that incorporate one or more crystallizable components have received continuing attention as they offer an effective route to novel property profiles.[3–8]

The Dow Chemical company has made olefin block copolymers (OBCs) via a process called chain shuttling polymerization.[9] These blocky copolymers comprise crystallizable ethylene–octene copolymer blocks with low octene content and high melting temperature (hard blocks), alternating with amorphous ethylene–octene copolymer blocks with high octene content and low glass transition temperature (soft blocks).[10] Details about the one-component OBC's phase behavior have been discussed in our previous study.[11] It was found that as the octene content increased, mesophase separation between hard blocks and soft blocks becomes more and more dominant and the crystal morphology degrades gradually from spherulites to dispersed and relaxed lamellar structures.

As for the iPP/OBC blends, the effect of OBCs' distinct molecular structure on the compatibility of iPP/OBC blends was also investigated systematically earlier.[12] The repulsion effect between the hard blocks and the soft blocks enhances mixing between iPP and OBC comparatively. This, coupled with the fact that the majority of soft blocks are more compatible with iPP as octene content increased, leads to better compatibility between iPP and OBC, which is proved by smaller dispersed domain size, better interfacial adhesion, and faster crystallization kinetics. On the other hand, we also found that annealing condition was important in controlling the superstructure of these blends.

It is well known that isotactic polypropylene (iPP) is used extensively owing to its stability, attainability, chemical resistance, low density, and so forth; however, straightforward method for the preparation of iPP morphologies with micro-

Table I. Characteristics of OBCs[a]

Sample	M_w (g/mol)	M_n (g/mol)	Net octene content (mol %)	Soft block octene content (mol %)	Hard block octene content (mol %)	wt. % of Soft segment
OBC1	180×10^3	76×10^3	17.9	22.6	1.1	84
OBC4	250×10^3	74×10^3	25.4	35.7	2.1	82

[a] Data were provided by the Dow Chemical Company.

sized iPP spheres of narrow size distribution was scarcely reported. In this study, we report a simple physical approach to obtain iPP structures with micro- and submicron spheres. According to the basic rules of phase separation, the diameter of the spheres could be adjusted by the compatibility of the blend and the annealing conditions. Meanwhile, bead–string spherulite could also be observed in the iPP/OBC system.

EXPERIMENTAL

OBCs synthesized by chain-shuttling technology were kindly supplied as pellets by the Dow Chemical Company. The molecular parameters of the OBCs used are listed in Table I. iPP (trademarked as S1003) with $M_w = 3.4 \times 10^5$ g/mol and $M_w/M_n = 3.8$ is a commercial product purchased from Beijing Yanshan Petrochemical. To tune the compatibility of iPP and OBC by changing the molecular weight of iPP, a lower molecular weight with $M_w = 1.3 \times 10^5$ g/mol and $M_w/M_n = 4.3$ (iPP^L, provided by the Dow Chemical Company) and a higher molecular weight iPP with $M_w = 85 \times 10^5$ g/mol and $M_w/M_n = 5.2$ (iPP^H, provided by Professor Dong Jinyong's research group in Institute of Chemistry of China Academy Science) were also used and blended with OBC1 with the weight ratio of 30/70 iPP/OBC, which are named as $1–70^L$ and $1–70^H$, respectively.

To prepare blends, iPP and OBC were dissolved in *n*-heptane with a polymer mass composition of about 1% at 130°C for 24 h, then coprecipitated from this hot *n*-heptane solution into a large excess of methanol at room temperature. After filtration, the polymers were dried in air for 24 h and further dried in a vacuum oven at room temperature for 3 days. An OBC weight fraction of 0.70 was used in these blends. Correspondingly, the OBC1/iPP blend (blend1) is designated as 1–70 and the OBC4/iPP blend (blend4) is designated as 4–70.

The optical microscopy (OM) observations were carried out using an Olympus (BX51) optical microscope and Olympus (C-5050ZOOM) camera. A Linkam (350) hot stage was used to control the experimental temperature. In a typical optical observation, a sample was heated to 200°C for 5 min to erase thermal history, and then quenched to 140°C for isothermal crystallization. Films (~30 μm) of the blends were prepared by hot pressing at 200 ± 2°C between two glass slides. For long-time annealing experiment at 200°C, the pressed specimens were surrounded with silicon oil to avoid thermal degradation of the polymer, and the nitrogen gas was also used to avoid thermal decomposition during the process.

The surfaces of samples after OM tests were etched in *n*-heptane at ambient temperature for at least 1 week to wash out the more soluble component of OBC, and then the film was coated with platinum prior to the examination by a scanning electron microscope (SEM). A JEOL (JSM 6700F) SEM was used with an operating voltage of 5 kV for this study.

RESULTS AND DISCUSSION

The whole profile of the isothermal crystallization structure of 1–70 and 4–70 at 140°C is shown in Figure 1. As shown in Figure 1(a), the "islands" of iPP-rich phase are dispersed in the "sea" of OBC-rich matrix, and a collection of these crystallized iPP "islands" are stacked together, forming a large irregular crystalline structure. As shown in the corresponding polarized optical micrograph on the right-hand side, it is clear that the iPP dispersed phase crystallized into the bright spots with birefringence. There is almost no typical sign of Maltese crosspattern, suggesting that the crystals are degraded seriously from spherulite structure. After crystallizing at 140°C for longer time as shown in Figure 1(b,c), the whole specimen was filled with these crystals without clear boundaries. Compared with the matrix before crystallization started, these irregular crystals make the phase-separated morphology much coarser so that it is much easier to distinguish the dispersed iPP-rich phase from the phase-contrast micrograph, and the crystalline morphology of iPP could be observed explicitly from the corresponding polarized optical micrograph. It appears that the iPP-rich phase is crystallized as discrete crystals individually as there are few connections between them.

For 4–70 shown in Figure 1(d), it presented a faster growth rate than 1–70 under this condition statistically, which could be easily concluded by comparing the average size of the crystals that formed during the same crystallization time. Meanwhile, the character of spherulite is preserved better in this situation as the typical Maltese cross can still be distinguished in the polarized optical micrograph. After crystallizing at 140°C for 2 h, the whole specimen is almost filled with spherulites, and the crystallized iPP "islands" are more continuous compared with 1–70. However, these spherulites are much more imperfect and relaxed than normal pure iPP as a great number of OBC molecules are incorporated in the interlamellar and/or interfibrillar regions during the crystallization process.

To explain the difference between these two blends, it is necessary to recall the conclusion of our previous study on iPP/OBC.[12] According to the results of our previous studies, it is known that the compatibility of iPP with OBC4 is much better than that with OBC1. Owing to the better compatibility with 4–70, it is believed that the iPP-dispersed domain size is smaller and there must be more iPP chains dispersed in the OBC matrix in 4–70 compared with 1–70 under the same annealing

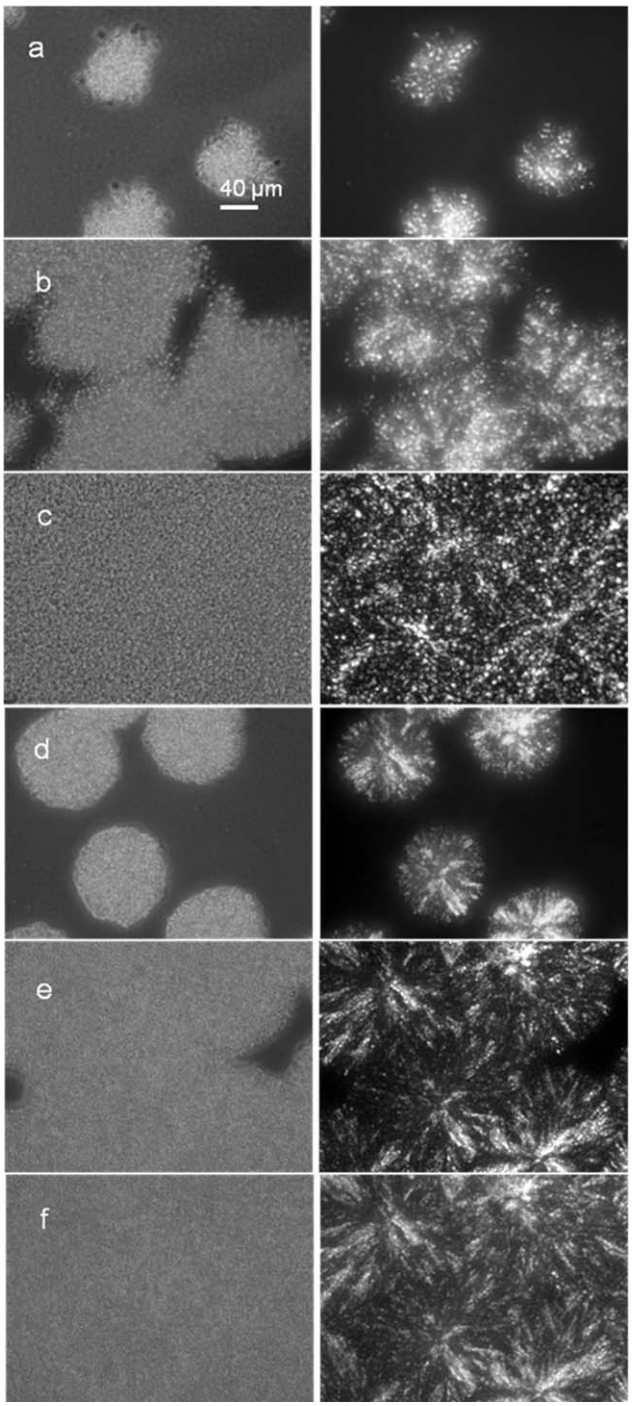

Figure 1. Optical micrographs of blends 1–70 and 4–70 crystallized at 140°C after annealing at 200°C for 5 min: (a) 1–70 crystallized at 140°C for 1 h; (b) 1–70 crystallized at 140°C for 2 h; (c) 1–70 crystallized at 140°C for 6 h; (d) 4–70 crystallized at 140°C for 1 h; (e) 4–70 crystallized at 140°C for 2 h; (f) 4–70 crystallized at 140°C for 6 h. The left-hand side images are the phase-contrast micrographs and those on the right-hand side are the polarized optical micrographs.

condition. During crystallization, these matrix-dispersed iPP chains could crystallize into lamellar stacks to serve as strings linking the isolated iPP beads together and enhancing the connection between these beads. As shown in Figure 1(d), it seemed that the growth in all radial directions is isotropic. Over time, plenty of domains were covered during the crystallization process, gradually forming spherulites with strings and beads. On the contrary, these strings in 1–70 are scarce in this situation as fewer iPP chains are distributed in the OBC1-rich matrix. As a result, the crystallization process is severely disturbed and much confined in the dispersed iPP-rich domains, and the growth of the crystal is so irregular and chaotic that a littery crystalline structure was obtained as shown in Figure 1(b,c).

To further elucidate the morphology of these two blends, the specimens after OM test were etched in *n*-heptane for 1 week at room temperature to wash out the more soluble OBC component. The SEM images of the etched blends are compiled in Figure 2, which shows the magnified area within an iPP spherulite or dendrite formed at 140°C.

The panorama view of 1–70 is shown in Figure 2(a). It is clear that there were a great many spheres in the whole specimen, and the iPP particles seem to be completely isolated in the OBC1 matrix as there were few links between them, and the dimension of these beads is not monodispersed as shown in the magnified image of Figure 2(b). If we further enlarge one bead with medium size, a detailed structure will be observed: the bead is a crystallized sphere with the typical lamellar structure.

For 4–70 [Figure 2(d)] an entire spherulite (dendrite) as well as fibrillar structures can be clearly observed. If we enlarge one part within the spherulite, the bead–string morphology is clearly unfolded, which is in good agreement with the results of OM as shown in Figure 1(d). To detect the refined structure of one bead in 4–70 and compare it with the isolated bead in 1–70, the magnified one bead is shown in Figure 2(f): the much coarser interface and more links between these beads could be observed. By comparing the iPP-rich domain size in Figure 2(e) with that in Figure 2(b), it is a little surprising to find that the dispersed domain size is larger in 4–70 than that in 1–70 at first sight, which is seemingly contradictory to our previous studies: as we mentioned before, the iPP domain size should be smaller in 4–70 than in 1–70 owing to the better compatibility between iPP and OBC4. Still, the interface factor should be taken into consideration: the diffuse interface between iPP and OBC4 makes the OBC4 component difficult to be washed out by solvent, resulting in much more OBC4 molecules remaining onto the beads in 4–70 under the same treatment as 1–70. Once the etching time was long enough for 4–70, iPP microspheres with smaller domain size and typical crosshatched lamellar structure can be obtained as shown in Figure 2(g,h). The crystal links shown in Figure 2(f) are evidences of the iPP strings in the OBC matrix linking the macrophase-separated iPP-rich domains within the spherulite (dendrite).

Figure 2 shows the crystallization morphology of the two blends after annealing at 200°C for 5 min. iPP microspheres were revealed under this condition. To control the dimension of the iPP microspheres, an annealing experiment was designed. Figure 3 shows the fast crystallization morphology of the two blends after annealing at 200°C for 12 h by rapidly quenching in liquid nitrogen. As shown in Figure 3(a), iPP-rich domains can be

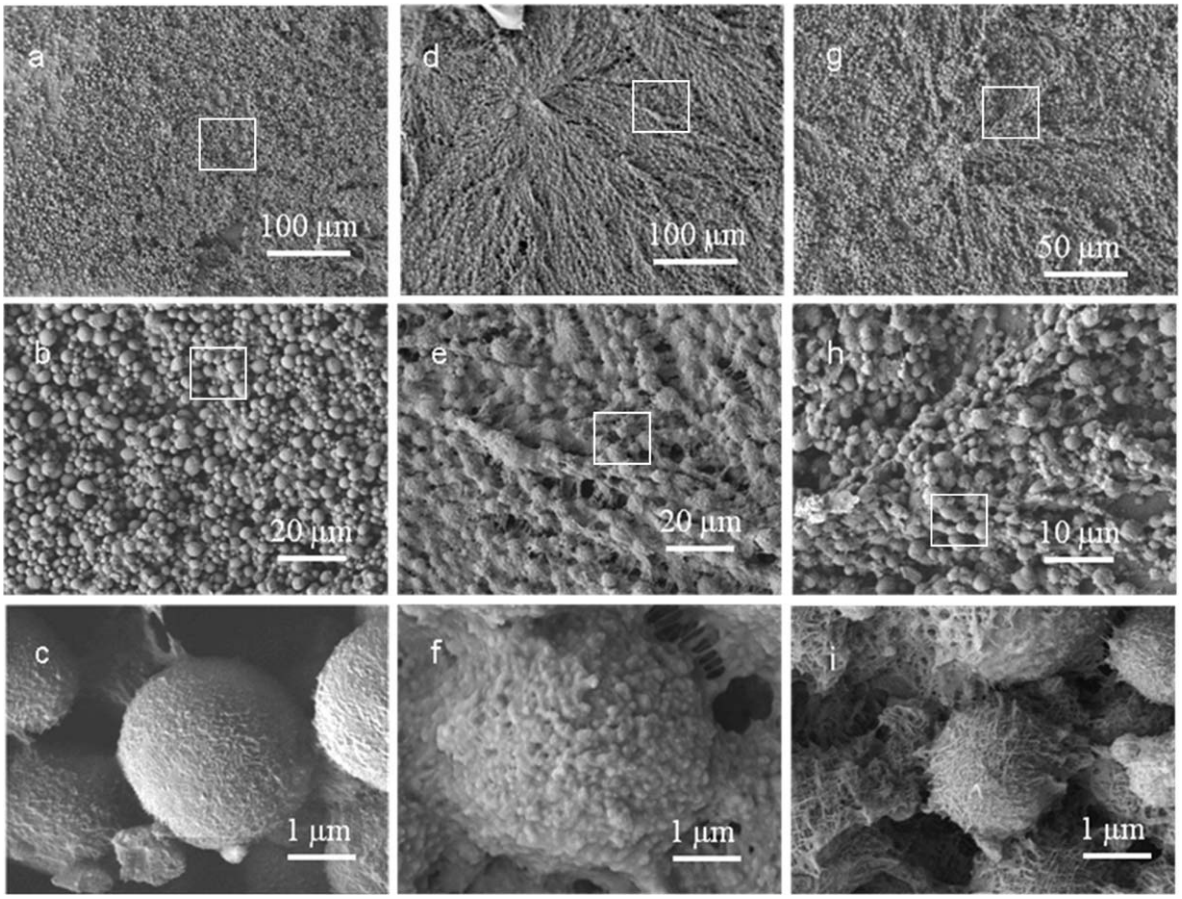

Figure 2. SEM images of the blends after crystallizing at 140°C for 6 h: the left panel is for 1–70, the other two are for 4–70. The lower two rows are the magnified images for the solid box in the upper one. The specimens were etched in *n*-heptane for 1 week in (a) and (d), whereas 2 weeks for the specimen in (g).

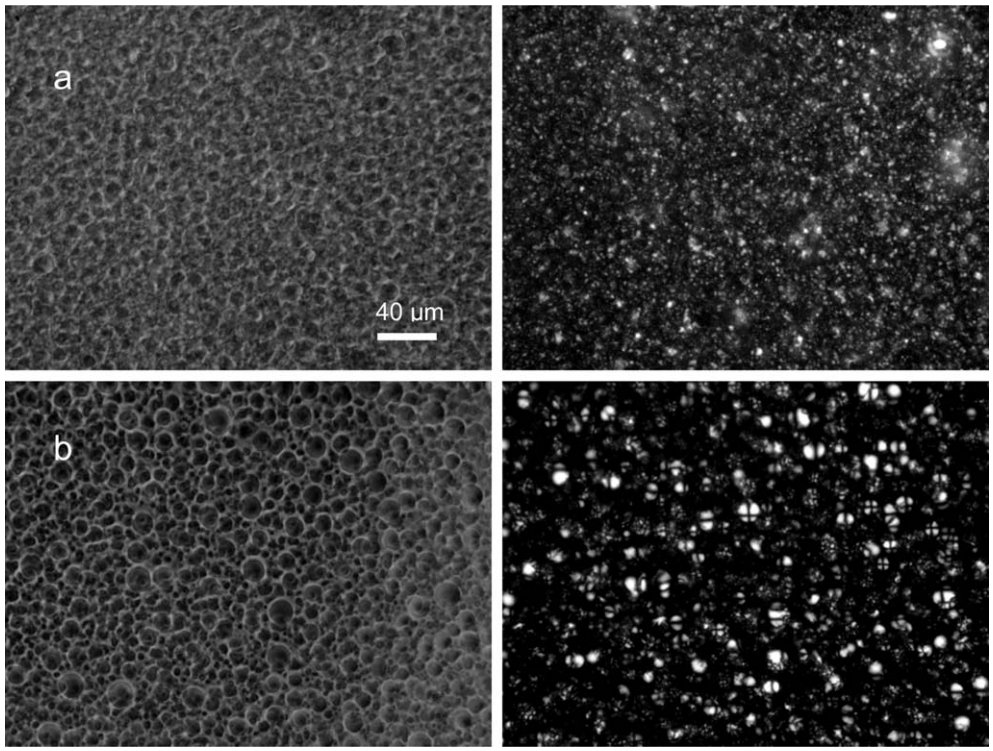

Figure 3. Optical micrographs of the two blends annealing at 200°C for 12 h followed by quenching in liquid nitrogen: (a) 1–70 and (b) 4–70. The left-hand side images are the phase-contrast micrographs and those on the right-hand side are the polarized optical micrographs.

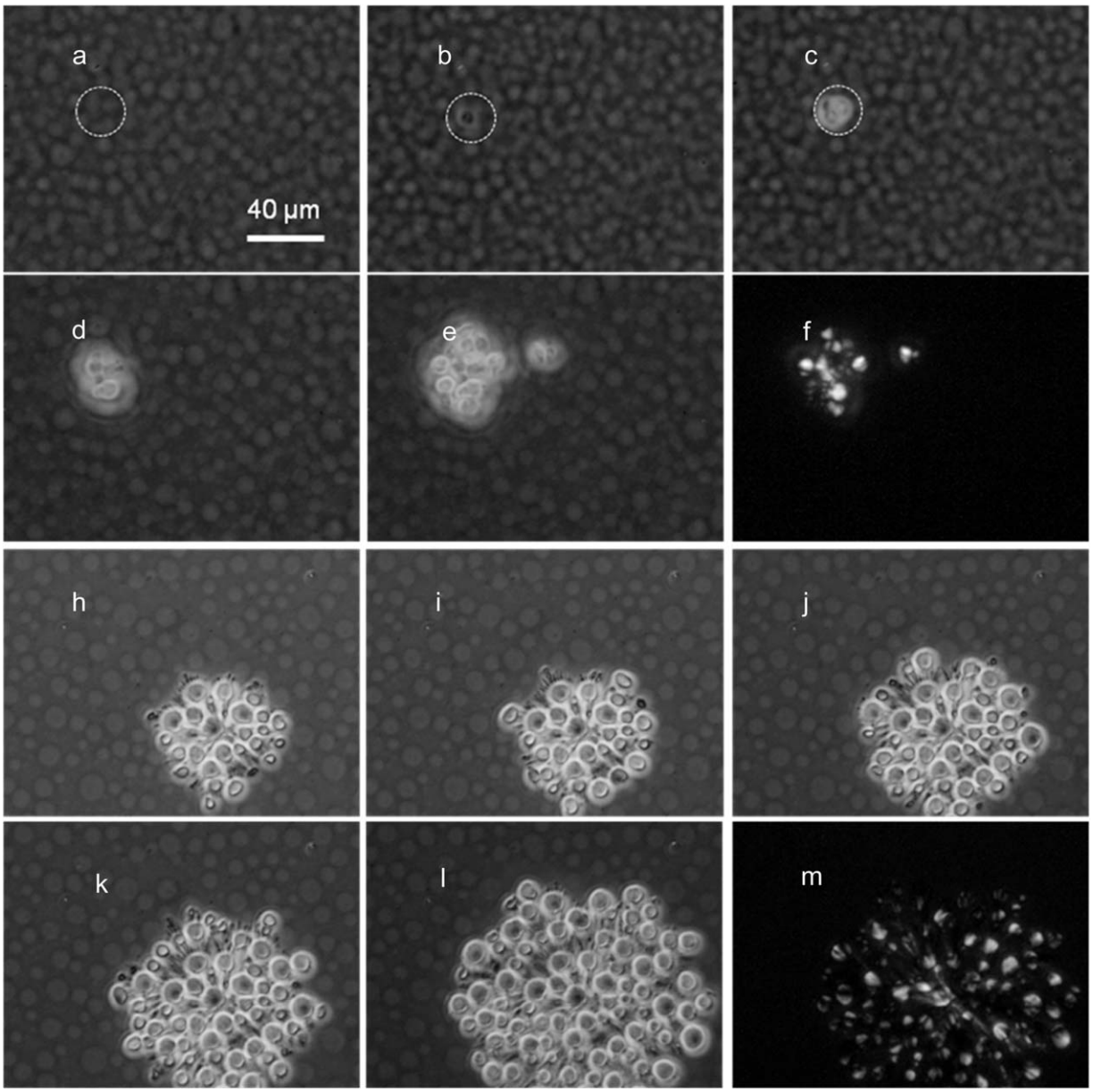

Figure 4. Optical micrographs of a time-resolved crystallization process of the two blends after annealing at 200°C for 12 h: (a–e) phase-contrast micrographs for 1–70 crystallized at 140°C. (a) 0 min, (b) 1 min, (c) 5 min, (d) 18 min, (e) 30 min, and (f) the corresponding polarized optical micrograph for (e); (h–l) phase-contrast micrographs for 4–70 crystallized at 140°C: (h) 30 min, (i) 33 min, (j) 41 min, (k) 47 min, (l) 60 min, and (m) the corresponding polarized optical micrograph for (l). The circles in shown (a–c) are drawn to guide the eyes for the iPP nucleus.

clearly resolved from the phase-contrast micrographs. Compared with Figure 1(c), we find that the size of iPP-rich domain greatly increased, however, in the corresponding optical-polarized micrograph, it is still not easy to distinguish the iPP-dispersed phase as both iPP and OBC1 have good ability to crystallize during the quench process.[11]

On the contrary, in Figure 3(b), the dispersed domains are very distinct both in the phase-contrast and in the phase-polarized optical micrographs. Furthermore, it is interesting to point out that there are some little spherulites with typical Maltese cross-pattern in the polarized optical micrograph formed even during rapid quenching in liquid nitrogen.

When comparing Figure 3(a) with Figure 3(b), it is confusing to find out that the domain size in 4–70 was almost the same or a little larger than that in 1–70, which is again seemingly contradictory to our previous results.[12] To explain this somewhat surprising result, spinodal decomposition kinetics were considered. To simply explain the situation, we could assume that all other parameters which would influence the phase-separation kinetics (such as the viscosity, the molecular weight, and so on) are equivalent in the two blends. It is well known that the dimension of the growing domains after spinodal decomposition follows $R(t) \sim t$ at the intermediate stage, and then changes into $R(t) \sim t^{1/3}$ in the later stage driven by the hydrodynamic coarsening and collision coalescence process,

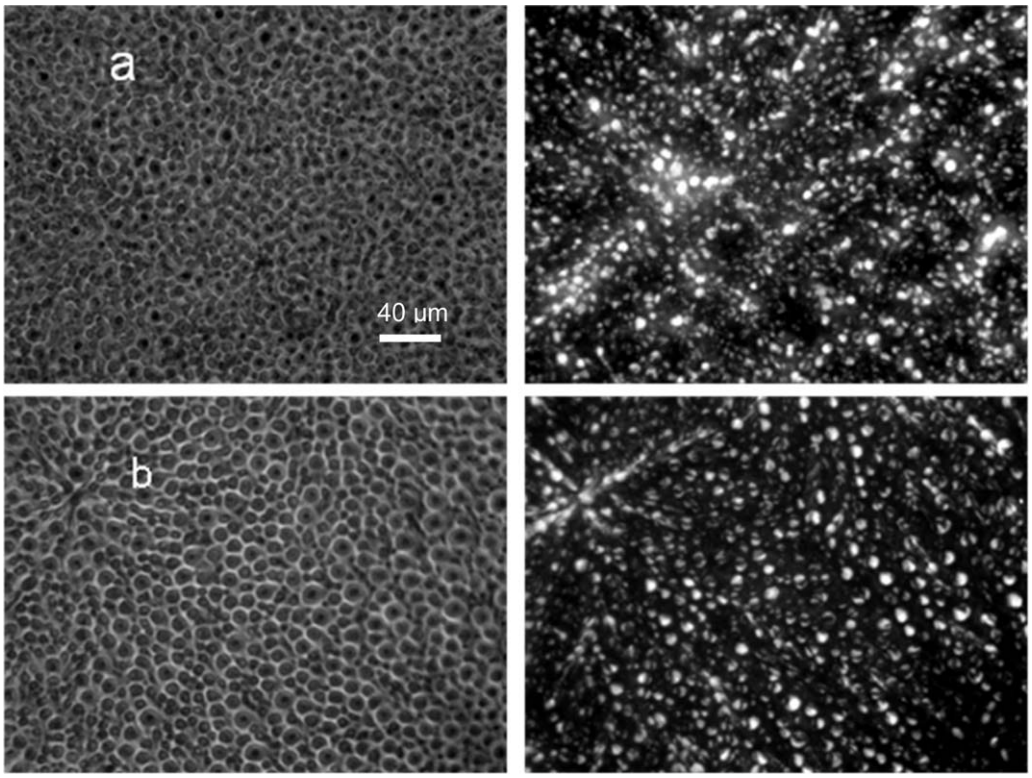

Figure 5. Optical micrographs of the two blends' crystallization at 140 °C for 6 h followed by cooling to room temperature at 10°C/min after annealing at 200°C for 12 h: (a) 1–70 and (b) 4–70. The left-hand side images are the phase-contrast micrographs and those on the right-hand side are the polarized optical micrographs.

respectively (we have shown that the two blends at 200°C are in the unstable region subsequently).[13,14] It is believed that the dispersed domain size is smaller in 4–70 when annealing at 200°C for shorter time owing to the better compatibility between iPP and OBC4. In other words, 1–70 is in the later stage of the phase separation than 4–70 as we have demonstrated before, which will follow the $R(t) \sim t^{1/3}$ coarsen rate earlier during the same annealing process at 200°C. Therefore, the intermediate spinodal decomposition stage could last for a longer time in 4–70, in which the kinetics of phase separation follows the $R(t) \sim t$ relationship. Taking this difference in phase-separation kinetics into consideration, it is reasonable to believe that the iPP-rich domain size is larger in 4–70 than in 1–70 after annealing for long enough. The other reason for the longer time of 4–70 stays in the intermediate stage is owing to a smaller interfacial tension and a slower breaking up of the cocontinuous intermediate structure due to the better compatibility.

To investigate the influence of deep macrophase separation on the following isothermal crystallization, the morphology of isothermal crystallization from the preformed phase-separation morphology was further studied. The crystallization process of 1–70 and 4–70 at 140°C after annealing at 200°C for 12 h was traced with time-resolved OM as shown in Figure 4. Figure 4(a) clearly shows the macrophase-separation morphology of 1–70 after annealing at 200°C for 12 h. The average dimension of the dispersed iPP-rich phase domain has grown up as large as 10 μm. As shown in Figure 4(b), a crystal nucleus formed after quenching to 140°C, and then the formed nucleus began to grow into the iPP-rich phase. By covering some more iPP-rich phase domains randomly around the nucleus, a large irregular crystal was formed. Meanwhile, another nucleus formed and grew. They will impinge with each other with time. From these time-resolved micrographs, it is intuitive to detect how the iPP-rich phase domains crystallize from the well phase-separated morphology. For 4–70 [Figure 4(h–m)] the dispersed domain size increased remarkably after annealing at 200°C for 12 h and a "bead–string" growth manner was clearly presented here. It is easy to see that the threads around the beads link the dispersed iPP crystalline domains together forming a spherulite (or dendrite) structure owing to the typical isotropic radial growth manner. To observe the final crystallization morphology of the two blends, Figure 5 shows the profile of these dendrites crystallized at 140°C for 6 h.

As shown in Figure 5, the crystals formed in 1–70 [Figure 5(a)] are jumbled together that no dendrite could be distinguished at all. iPP crystallized mainly in its own rich phase, the dimension of the domain size increased to about 10 μm in average after phase separation at 200°C. For 4–70, the domain size of iPP-rich is comparable to or a little larger than that in 1–70 as described before. Although the Maltese crosspattern is degraded a lot in this case, there are still traces of the strings linking the dispersed iPP-rich domains, and the spherulite structure was preserved in 4–70 under this condition.

By comparing Figure 1 with Figure 5, the iPP sphere domain size could be tuned from 1 μm to more than 10 μm through

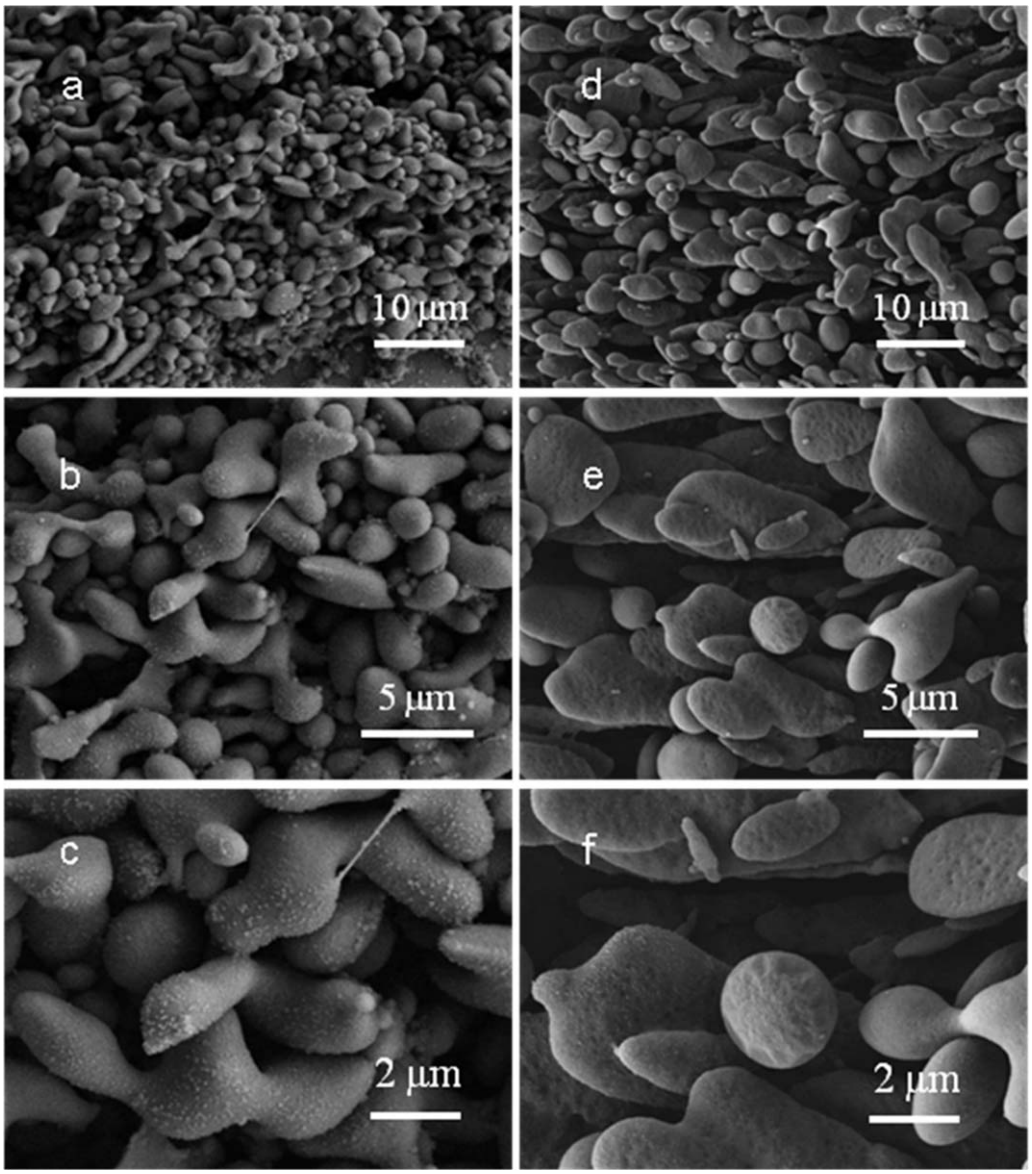

Figure 6. SEM images of the two blends annealing at 200°C for 5 min followed by quenching into liquid nitrogen: (a–c) for 1–70; the other three are for 4–70. The samples were etched in *n*-heptane for 1 week after removing the cover glass in liquid nitrogen.

simple annealing. It is necessary to find out the mechanism of the formation of these microspheres. As we know that quenching experiment is usually an ideal approach to target a phase-separation structure as the crystallization could be a much faster process to freeze the initial morphology of phase separation. Figure 6 shows the phase-separation morphology of the two blends annealed at 200°C for 5 min followed by rapid quenching into liquid nitrogen. The left column is for 1–70, whereas the right one is for 4–70.

In Figure 6(a), the phase-separation morphology is typical for the spinodal decomposition type which exhibits a broken structure from interconnected morphology. In the enlarged image of Figure 6(b), the iPP-rich domains with the irregular form were presented. Obviously, some large-scaled structure about 5 μm in length was breaking up at the position with the largest curvature to reduce the surface energy,[13] which is more typical as shown in Figure 6(c). These images vividly showed the process of breaking up from the interconnected into the sea–island structure with the isolated iPP-rich phase distributed in OBC1 matrix in 1–70. In contrast, the thin sheet structure which had been reported to be one of the original bicontinuous structure is dominant in 4–70.[14] As shown in Figure 6(d), there are discrete spheroids besides the sheet structure. In the magnified images of Figure 6(e,f), it is obvious that the sheets are also breaking up at the positions with greatest curvature.[13] According to the morphology obtained at the very beginning of the phase-separation stage, it can be concluded that the isolated microspheres of iPP are evolved from the irregular interconnected or the sheet structure along with annealing and/or during the cooling to the crystallization temperature.

Based on the previous results, it was verified that the original morphologies of the two blends are both representative of

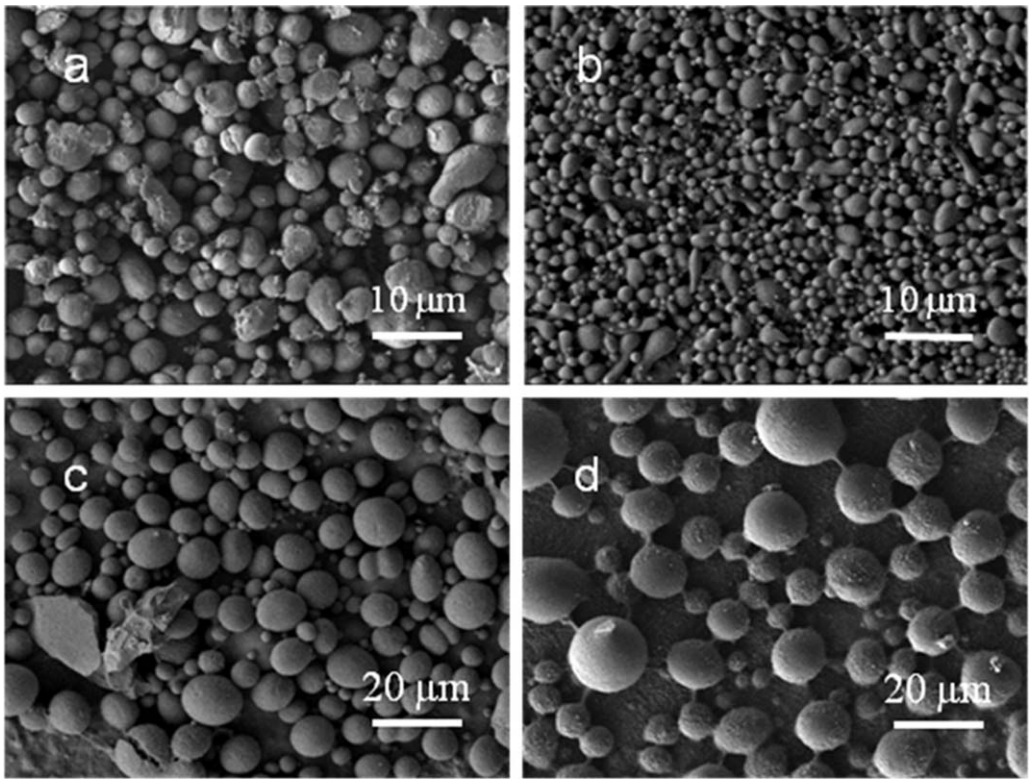

Figure 7. SEM images of the two blends cooling to room temperature at 10°C/min after annealing at 200°C for 5 min: (a) 1–70; (b) 4–70; and 12 h: (c) 1–70 and (d) 4–70. The samples were etched in *n*-heptane for 1 week after removing the cover glass in liquid nitrogen.

spinodal decomposition as shown in Figure 6, which indicates that the iPP beads are formed not only in the process of annealing at 200°C for 5 min, but also during the cooling to 140°C or/and isothermal process at 140°C as well. To obtain microspheres through a much simpler way, Figure 7 shows the results that the samples were directly quenched from the molten state after annealing at 200°C to room temperature at a certain rate. In Figure 7(a,b), we show the results of cooling the blends to room temperature at 10°C/min after annealing at 200°C for 5 min. It is obvious that both blends can form isolated iPP-rich spheres; even, there are some domains with a bone shape or some other irregular forms in the two blends. It can be speculated that the irregular spinodal decomposition structure broke into isolated iPP-rich domains during the cooling, and the threads linking the iPP-crystallized beads will be weaken during the faster nonisothermal crystallization process. If the strings in the spherulite are decreased, microspheres of iPP can be easily obtained as shown in Figure 7(b). From these results, it can be concluded that isothermal crystallization is not a necessary condition for the formation of the iPP microspheres.

Figure 7(c,d) shows the morphology of the two blends' nonisothermal crystalline structure after annealing at 200°C for 12 h. During the annealing, the interconnected phase structure broke into isolated iPP-rich domains within the OBC-rich matrix and the iPP-dispersed domains coarsen into larger ones during the

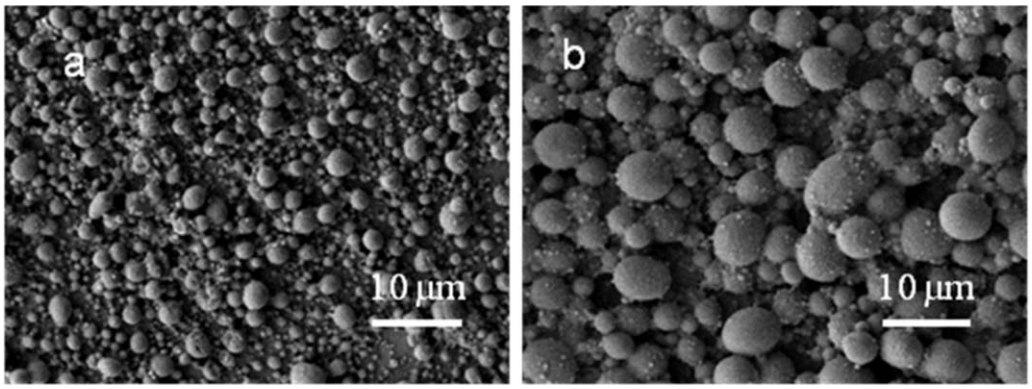

Figure 8. SEM images of blends cooling to room temperature at 10°C/min after annealing at 200°C for 5 min: (a) 1–70L and (b) 1–70H. The samples were etched in *n*-heptane for 1 week after removing the cover glass in liquid nitrogen.

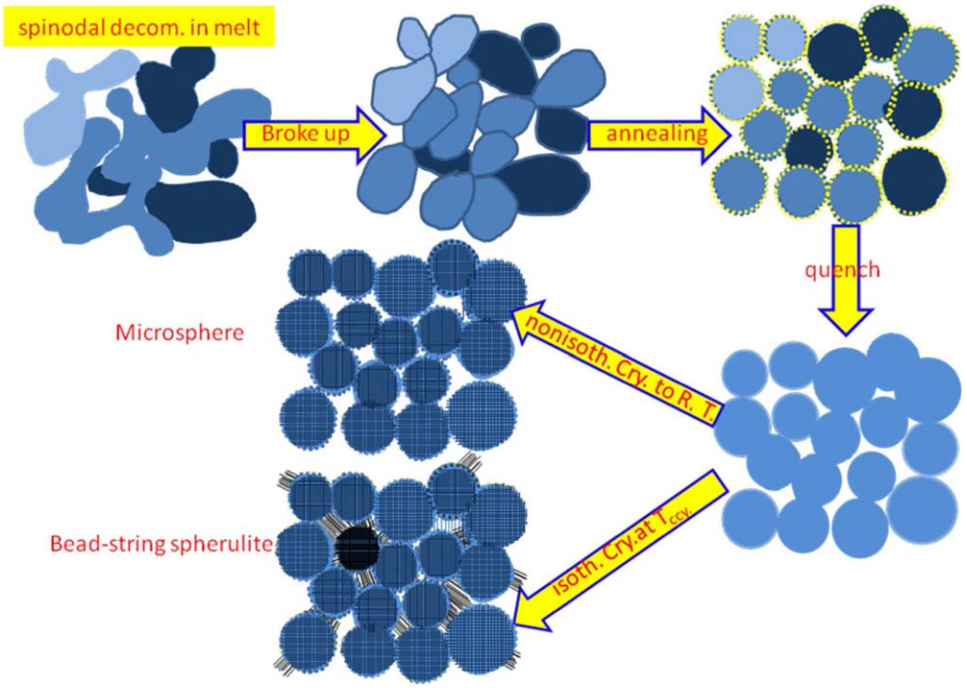

Figure 9. Illustration sketches for the formation of iPP microspheres and bead–string spherulite in iPP/OBC blends. The yellow-dashed circles highlight the isolated microsphere domains. [Color figure can be viewed in the online issue, which is available at wileyonlinelibrary.com.]

further annealing. Through cooling to room temperature, the dispersed iPP domains would quickly crystallize in their own rich phase. After etching the matrix of OBC, the iPP domains come out as shown. Even after phase separation at 200°C for 12 h for 4–70, the connectivity between the crystallized iPP beads can still be observed during the nonisothermal crystallization as shown in Figure 7(d). As discussed before, the larger domain size of 1–70 in Figure 7(a) originated from the poor compatibility between OBC1 and iPP, whereas the larger domains in Figure 7(d) resulting from the longer range of coarsening time in the faster hydrodynamic coarsening region owing to the smaller interfacial tension for this more compatible system.

We have shown that iPP microsphere structure is obtained through spinodal phase separation, and the dimension of these microspheres can be controlled by tuning the compatibility and the annealing condition. Meanwhile, it is known that the Flory–Huggins free energy of a binary mixture ΔF is a function of temperature, composition, and molecular weight in the blend.[15] Therefore, the molecular weight of either component of the blends is expected to be another effective factor which can affect the compatibility in blends, whereas the other parameters are fixed. To determine the influence of molecular weight of iPP on the dimension of the iPP microspheres, iPP^L and iPP^H were selected to blend with OBC1, which are named as $1–70^L$ and $1–70^H$, respectively (with composition of 30/70 iPP/OBC1). Figure 8 shows the results of $1–70^L$ and $1–70^H$ nonisothermally crystallized at 10°C/min after annealing at 200°C for 5 min. Comparing Figure 8(a) with Figure 8(b) as well as Figure 7(b), it is obvious that the dimension of the spheres in the blend with the higher molecular weight iPP is two or three times larger than the one with the lower molecular weight, which indicates that changing the molecular weight is effective in tuning the dimension of the iPP spheres.

Based on the results shown above, the formation of iPP microsphere structure and bead–string spherulites in iPP/OBC blends from spinodal decomposition is schematically shown in Figure 9. The initial bicontinuous structure broke up into dispersed domains, and then these domains with irregular shape evolved into sphere ones under the driving force of lowering the surface tension. The dimension of these iPP microspheres could be tuned by annealing condition or/and compatibility of the blend from 1 μm to more than 10 μm in average.

CONCLUSIONS

iPP microspheres with diameters ranging from 1 μm to more than 10 μm are obtained by adjusting compatibility and annealing condition in iPP/OBC blends. In addition, molecular weight is another effective way to tune the morphology in blends: the dimension of the iPP microspheres could be reduced/increased by blending OBC with a lower/higher molecular weight iPP component, respectively. The molecular structure of OBC, the molecular weight of iPP, as well as the annealing condition are scalable in tuning the dimension of the iPP microspheres. As to the mechanism of the formation of iPP microspheres, the original morphology was found to be spinodal decomposition with interconnected morphology or thin sheet structure. The microspheres are prepared by the process of breaking up from the irregular structure and the subsequent coarsening. Based on the morphology formed by phase separation in the molten state,

iPP microspheres could be obtained both in the process of isothermal crystallization and in the nonisothermal crystallization. In addition, during the isothermal crystallization, a spherulite with bead–string structure could be obtained.

ACKNOWLEDGMENTS

This study was supported by National Natural Science Foundation of China (No. 50930003) and Young Scientist Fund of NSFC (No. 21004071). The authors thank the Dow Chemical Company for kindly providing the samples of OBC and iPP^{L}. One of the authors Jin Jing appreciates Niu Hui for providing the higher molecular weight iPP^{H}.

REFERENCES

1. Paul, D. R.; Newman, S. Polymer Blends; Academic Press: New York, **1978**.
2. Utracki, L. A. Polymer Alloys and Blends; Hanser Publishers: New York, **1989**.
3. Vilay, V.; Mariattia, M.; Ahmad, Z.; Pasomsouk, K.; Todo, M. *Mater. Sci. Eng. A* **2010**, *527*, 6930.
4. Du, J.; Niu, H.; Dong, J.; Dong, X.; Han, C. C. *Adv. Mater.* **2008**, *20*, 2914.
5. D'orazio, L.; Mancarella, C.; Martuscelli, E.; Sticotti, G. *J. Mater. Sci.* **1991**, *26*, 4033.
6. Lohse, D. *J. Polym. Eng. Sci.* **1986**, *26*, 1500.
7. Barlow, J. W.; Paul, D. R. *Polym. Eng. Sci.* **1981**, *21*, 985.
8. McNally, T.; Mcshane, P.; Nally, G. M.; Murphy, W. R.; Cook, M.; Miller, A. *Polymer* **2002**, *43*, 3785.
9. Arriola, D. J.; Carnahan, E. M.; Hustad, P. D.; Kuhlman, R. L.; Wenzel, T. T. *Science* **2006**, *312*, 714.
10. Shan, C. L. P.; Hazlitt, L. G. *Macromol. Symp.* **2007**, *257*, 80.
11. Jin, J.; Du, J.; Xia, Q. H.; Liang, Y. R.; Han, C. C. *Macromolecules* **2010**, *43*, 10554.
12. Jin, J.; Zhao, C. Z.; Du, J.; Han, C. C. *Macromolecules* **2011**, *44*, 4326.
13. Binder, K. *Colloid Polym. Sci.* **1987**, *265*, 273.
14. Hashimoto, T.; Kumaki, J.; Kawai, H. *Macromolecules* **1983**, *16*, 641.
15. Hasegawa, H.; Sakurai, S.; Takenaka, M.; Hashimoto, T.; Han, C. C. *Macromolecules* **1991**, *24*, 1813.